

SCATTERING PROPERTIES OF INTERSTELLAR PARTICLES

I. DIFFUSE GALACTIC RADIATION

ADOLF N. WITT

Yerkes Observatory

Received July 12, 1967; revised September 18, 1967

ABSTRACT

New photoelectric measurements in three band passes centered at $\lambda\lambda 3600, 4350$, and 6100 \AA of the intensity and distribution of the diffuse radiation in the Galaxy in the constellations of Cygnus and Taurus-Auriga are presented. Contaminations originating in other sources of light in the night sky have been investigated and are taken into account. The residual intensity is interpreted as general galactic starlight scattered by interstellar dust particles. A model for the radiative transfer of direct and scattered starlight in our Galaxy is discussed, and parameters related to the distribution of stars and dust are derived. Scattering properties of the interstellar particles are determined by comparing the observations with model computations of the intensity of the diffuse galactic radiation for various values of the albedo and the asymmetry of the phase function of the particles. The result of this study is that interstellar scatterers have an albedo close to unity and an isotropic phase function over the observed wavelength range. The observations rule out particles consisting of dirty ice, pure graphite, or graphite covered with a shell of ice as long as their scattering properties are described by the classical Mie theory for spherical isotropic particles. Quantum mechanically scattering particles as suggested by Platt are expected to exhibit characteristics in agreement with our observations.

I. INTRODUCTION

There is evidence for the existence of solid particles in the interstellar space from the observation of interstellar extinction, interstellar polarization, and from the spectra of reflection nebulae. In interacting with these particles, general galactic starlight is scattered in part, giving rise to a diffuse radiation field in our Galaxy. We refer to this as the diffuse galactic radiation (DGR).

The nature of interstellar particles has been explored observationally following two major approaches, the study of the transmitted starlight and the study of the diffusely scattered light. While the first has been dealt with in extensive extinction and polarization observations, the latter suffered from great inherent difficulties; one has to measure a low-intensity radiation on a much brighter sky background consisting of several components which vary with time and direction, and one has to have knowledge about the geometric relationship between the illuminating source and the scattering medium.

Since the problem of geometry seems to be relatively simple in the case of the Galaxy as a whole compared with that of an individual reflection nebula, accurate measurements of the intensity and distribution of the DGR promise to provide the most certain information on the scattering properties of interstellar dust particles.

The two parameters to be derived from the observations are the albedo of the particles and the asymmetry of the phase function governing the scattering of starlight by particles and their respective dependences on wavelength. Various models for interstellar particles differ greatly in these two parameters; therefore, a distinction among different particle models will be possible on the basis of accurate data on the DGR.

Following a theoretical study by Wang Shih-ky (1936) and the first photoelectric measurements by Elvey and Roach (1937), a detailed photographic examination of the DGR in two regions of the Milky Way was carried out by Henyey and Greenstein (1941) at the Yerkes Observatory. They concluded that interstellar particles consist of strongly forward-scattering grains with a relatively high albedo. Their measures were subject to uncertainties arising from insufficient knowledge of the faint-star background and from

the photometric techniques employed at the time, making the conclusion a rather tentative one.

Considerable doubt was cast upon their results in a critical discussion by van Houten (1961) based on photoelectric photometry of the night-sky by Elsässer and Haug (1960). There is evidence, however, that the latter work suffers from systematic calibration errors as indicated by Roach (1964), leaving the question of the DGR in a very uncertain state.

A new observational program for photoelectric measurements of this radiation in three band passes was initiated for this reason; simultaneously, the data obtained were intended for independent observational tests of some models for interstellar particles, which have been suggested recently. The object of this work is to investigate the most likely physical properties of interstellar particles based on observations of their scattering behavior.

The measurements were carried out at the McDonald Observatory during November and December, 1965, and June and July, 1966. The outstanding advantage of this observing site is its isolated location, which assured complete absence of sky brightening

TABLE 1
APPROXIMATE SECTIONS OF THE MILKY WAY
COVERED BY THE OBSERVATIONS

TAURUS-AURIGA		CYGNUS	
b^{II}	l^{II}	b^{II}	l^{II}
+30° .	152°-185°	+30° . . .	66°-76°
+20 . .	158 -185	+20	65 -74
+10 . .	163 -178	+10	64 -72
+ 5	166 -175	+ 5	66 -72
0	171 -176	0	69 -73
- 5	170 -178	- 5	69 -78
-10	169 -178	-10	70 -80
-20	166 -173	-20	71 -89
-30	157 -170	-30	79 -89

by artificial sources, while the low geographic latitude and the closeness of a minimum of solar activity reduced the possibility of aurora.

II. OBSERVATIONS

During astronomically dark hours at a suitable observing site, the primary sources of the night-sky brightness are starlight, zodiacal light, night airglow, and the diffuse galactic light. The last of these is to be measured with the least amount of disturbing influence from the other sources. In preparing the observing program some guidelines set forth by Henyey and Greenstein (1941) were followed.

In order to detect the distribution of the DGR with respect to galactic latitude, observations at well-distributed points reaching to about 30° on either side of the galactic equator were planned. A complete series of observations along an arc of about 60° length was to take approximately 5 hours. About thirty points along this arc had to be observed. In addition, all successive measurements had to be carried out at about the same zenith distance in order to eliminate the zenith distance dependence of the airglow, thus leaving only an azimuthal variation for this contribution, which here is assumed to be negligible, and a time dependence, which can be determined during a given night by proper monitoring measurements.

Coordinates satisfying these conditions were computed for two regions of the Milky Way—the constellations of Cygnus and Taurus-Auriga—for the two respective observing seasons. These two general directions coincide with those of Henyey and Greenstein (1941). In Table 1 we have listed the approximate boundaries of the chosen Milky Way sections in order to facilitate the comparison with other investigations. For each of the areas, coordinates along four separate arcs were found and the BD star closest to each of the points was chosen as reference center. From inspection of the *Palomar Sky Survey* prints it was apparent that in the immediate neighborhood of each of these stars—within a radius of $3'-4'$ —circular fields could be found which in all but a few cases were free of stars even as faint as $m = 20$, provided the diameter of these fields was smaller than about $70''$. Therefore, fields of $67''$ diameter were selected and their coordinates relative to the reference stars were measured. In this fashion it could be expected that the faint-background-star contribution would be reduced to a very small amount while at the same time the fields were still large enough to contain sufficient light—equivalent to a star of about $B = 14$ —to be measured accurately with a large telescope in the allotted time.

Special attention was given to the condition that the fields should be representative of general interstellar space and not be preferentially located on dust lanes or dark nebulae. A cross-check with B. Lynds's (1962) catalogue of dark nebulae confirmed that no more fields than could be expected from pure chance coincidence were associated with dust concentrations.

The program was carried out as described above with the 82-inch Otto Struve and the 36-inch telescopes of the McDonald Observatory. The three band passes employed were defined by the following filters and multipliers: the standard U and B filters of the UBV system with a 1P21 multiplier and an interference filter centered at $\lambda 6100 \text{ \AA}$ with 275 \AA half-width in combination with an ITT 130-G multiplier (S20 response). The last of these will be called "ORANGE" throughout the following. These filters provided a wide wavelength base and at the same time excluded major night-sky air glow. The ORANGE filter had a rectangular transmission profile and was therefore hardly influenced by the airglow emission $\lambda\lambda 6300$ and $5890-5896 \text{ \AA}$. Circular diaphragms were placed in the focal planes of the telescopes limiting the diameter of the fields to $67''$ in both cases. The photometers were equipped with an offset guider allowing accurate displacements (error in setting $0''.7$), thus making it possible to measure precisely the preselected fields during repeated runs once the telescope was pointed toward the reference stars. The offset guider and the 1P21 photometer were designed by W. A. Hiltner; the ITT 130-G photometer was constructed by C. R. O'Dell. A d.c. chart recorder system and a 1-Mc pulse-counting system were both used as recording devices during the program.

Measures during a given night were always made in pairs of band passes in the combinations of either U and B or U and ORANGE. The color which could thus be derived was an additional check on whether starlight was accidentally included in the field, since its contribution enters primarily at the band pass with the longer wavelength. The red leak of the U filter, which was especially serious in measurements with the ITT 130-G multiplier, was recorded in all cases.

The time variation of the night airglow was determined from hourly observations at the north pole of the sky. This interval was found to be sufficient owing to the fact that during good photometric nights the sky brightness varied only slowly with time. The atmospheric extinction in a given night was derived from observations of standard stars through varying air mass, the same observations serving also for calibration of all measurements into the standard photometric system. In addition to the U and B magnitudes, which were taken from the UBV system, the ORANGE magnitude had to be newly defined. This definition was accomplished by measuring a large number of UBV standard stars of different colors with the $\lambda 6100 \text{ \AA}$ filter-ITT 130-G multiplier combination and by assuming that for A0 V stars the relationships $B - \text{ORANGE} = 0.0$ and $U - \text{ORANGE} = 0.0$

are valid. These data were used later for the additional purpose of describing the general luminosity function of the solar neighborhood in terms of ORANGE magnitudes.

The reduction of the observations consisted of several steps. The extinction and the scattering by the lower atmosphere are assumed to be functions of zenith distance only for a given band pass. The extinction is determined in the usual manner from measures of standard stars; in correcting for it one adds a constant fraction of the measured intensity at any point. The scattering correction is obtained by multiplying the intensity of the total radiation in the respective band pass incident at the top of the atmosphere, averaged over the hemisphere of the sky with the value of the scattering function for the respective zenith distance. This constant amount is subtracted from all measured intensities. For the values of the scattering function the tables of Ashburn (1954) were used which are based on Chandrasekhar's (1950) rigorous solution for a Rayleigh scattering atmosphere; zero ground albedo was assumed and the height of the emitting layer was taken to be infinite. It was found that it was not necessary to correct separately for scattered airglow which originates at a finite height of about 100 km or to assume a higher value for the ground albedo, since the final DGR intensities derived from the described reduction were identical to the intensities obtained when the original Henyey-Greenstein reduction method was applied. Their procedure does not explicitly correct for scattered light but derives values for the DGR intensity by correcting only the amounts above an assumed zero level at $b^{\text{II}} = 30^\circ$ for extinction, since the zero level for constant zenith distance already contains all scattered light.

In our reduction the reduced intensities still contain contributions mainly from airglow, zodiacal light, and faint stars in addition to the DGR. At high galactic latitudes the first two are the dominant sources. Since the measurements are obtained at points up to more than 30° on either side of the galactic equator we can thus establish the combined brightness of these contributions at higher latitudes, and it is not a difficult task to also interpolate the height of this brightness level for the vicinity of the galactic equator. This is simplified by the fact that all measurements were performed at constant zenith distance. Once the airglow is corrected for time variations the only changes in the combined level are due to differences in the brightness of the zodiacal light along the arc crossing the Milky Way.

Data on the zodiacal light were taken from the work of Smith, Roach, and Owen (1965). Corrections for the gegenschein were based on isophotes determined by Elsässer and Siedentopf (1957). The Cygnus measurements avoided the zodiac sufficiently so that the level of airglow combined with zodiacal light hardly varied; in Taurus, however, detailed corrections for the gegenschein were required.

The approach of Henyey and Greenstein (1941) has then been followed by assuming that the radiation detected above the level of airglow and zodiacal light at lower galactic latitudes is due primarily to the DGR with a small contamination originating in starlight.

In cases where stars brighter than $m = 20$ could not be excluded from the fields an estimate of their contribution had to be made. By inspection of the *Palomar Sky Survey* prints the approximate magnitude of the brightest star in the field was found and the determination of the faint starlight started from this limit. The faint-star contribution was based on the extrapolation of existing star counts in the general direction of the observations—for Cygnus counts by Miller and Hynek (1939), for Taurus counts by McCuskey (1938)—and the relative size of the corrections for the different band passes was derived from a theoretical model of the Galaxy, which will be described in a later section. The contribution of stars fainter than the *Palomar Sky Survey* limit (a correction which had to be applied to all measurements) was evaluated on the same basis. This correction was found to be small as long as the luminosity function is similar to that of the solar neighborhood and the average linear extinction coefficient exceeds 1 mag/kpc. The relative size of the various components of the measured radiation is shown in Table 2,

which contains representative values for the galactic equator in Cygnus. The units are numbers of A0 V stars of $V = 10.0$ per square degree in the respective band pass.

Regions of the Milky Way showing any traces of gaseous emission on the red plates of the *Palomar Sky Survey* have been generally avoided in the measurements with very few known exceptions. These few exceptional points received low weights in the final interpretation of the data and it can therefore be assumed that the results are not significantly influenced by contributions due to diffuse-line emission originating in gaseous nebulae.

We thoroughly investigated the question of light coming from stars just outside the field of measurement, which may enter into the field by scattering in the telescope and by narrow-angle forward scattering in the atmosphere. Observational tests with the equipment and telescopes used showed that in an average star field this effect adds less than 1 per cent to the intensity finally interpreted as DGR. This is insignificant in view of the over-all uncertainties arising from other corrections.

TABLE 2
INTENSITY OF VARIOUS LIGHT SOURCES NEAR THE
GALACTIC EQUATOR IN CYGNUS*

Source	U	B	ORANGE
Airglow and zodiacal light ..	140	80	225
DGR..... ..	45	40	90
Faint stars $B > 17$	5	9	40
Faint stars $B > 20$	1	2	6
Total star background..	160	170	500

* The units are numbers of A0 V stars of $V = 10.0$ per square degree in the respective band pass.

After calibration, the intensities were converted into more convenient units of the number of A0 V stars of $V = 10.0$ per square degree in the band pass under consideration. As pointed out before, at higher galactic latitudes the recorded intensity can be assumed as being due primarily to airglow and zodiacal light; the DGR makes a significant contribution only at lower latitudes. We therefore introduced a zero level at $|b^{\text{II}}| = 27^\circ$, which is still well determined by the data, and considered only the intensities above this level which are at lower galactic latitudes.

These intensities for three band passes in Cygnus and for two in Taurus-Auriga are plotted versus galactic latitude b^{II} in Figure 1, *a-e*. It should be strongly emphasized at this point that at $|b^{\text{II}}| = 27^\circ$ there may still be a finite amount of DGR, the size of which depends mainly on the scattering properties of the dust medium. This, however, is the subject of this investigation, and no assumption or estimate will be made here except to note that the plotted intensities are not absolute values but that in each of the plots an additive constant is missing. We also conclude that in the interpretation of the data a method has to be chosen which takes into account this difficulty.

In each of the plots, results from up to four scans across the Milky Way are shown; in Cygnus each of the scans was observed several times while the Taurus-Auriga data should be considered less reliable because of marginal observing conditions and interference by the gegenschein. For this reason, much greater importance will be attributed to the Cygnus data. Features to be noted are the broadness of the distributions and the fact that the maxima do not exactly coincide with the galactic equator. The latter is due to local irregularities in the dust distribution as manifested by the great Cygnus rift and the Taurus dust complex.

III. THEORY

In order to quantitatively relate the measured intensities and distribution of the DGR with known properties of the galactic system and the unknown scattering characteristics of the interstellar dust, a Galaxy model is required.

The first aspect to be considered is that of the transfer of radiation in the Galaxy. Let us approximate the galactic system by a slab of scattering and emitting matter stratified along parallel planes, with an optical thickness $2\tau_1$ perpendicular to the planes, as given in Figure 2. Assume the position of the Sun to be in the central plane. Let the scattering

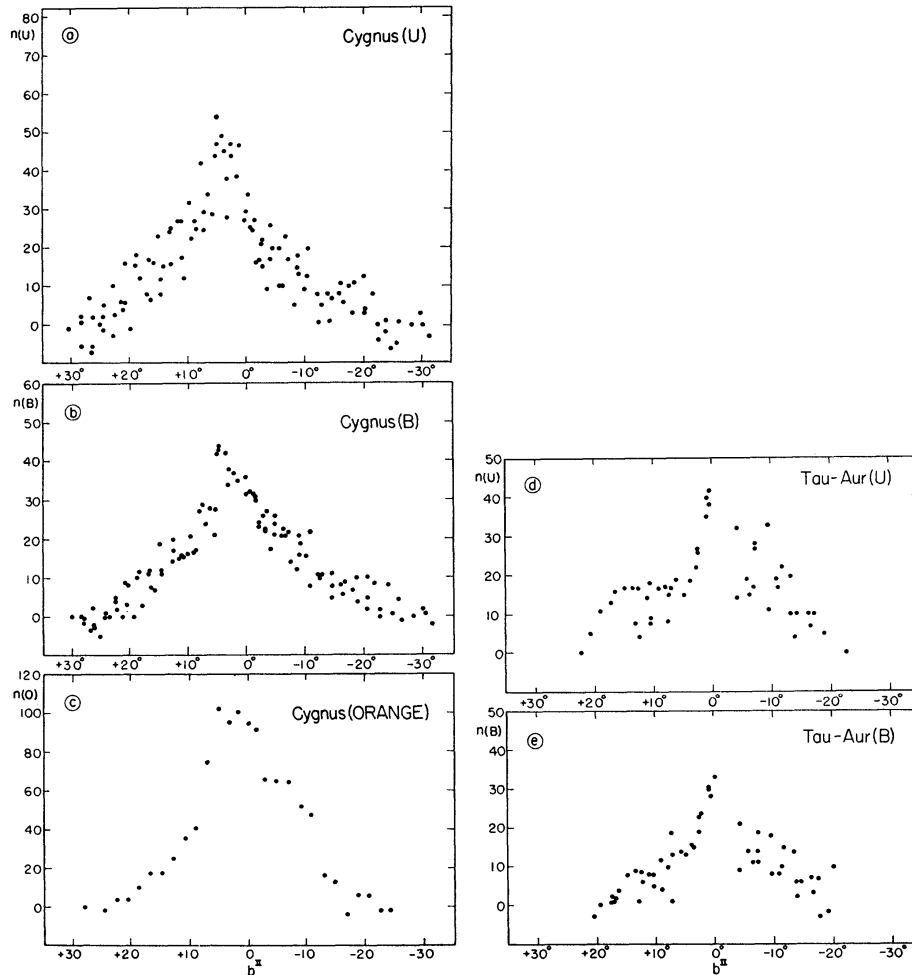


FIG. 1.—Observed DGR intensity distributions. The units are numbers of A0 V stars of $V = 10.0$ per square degree.

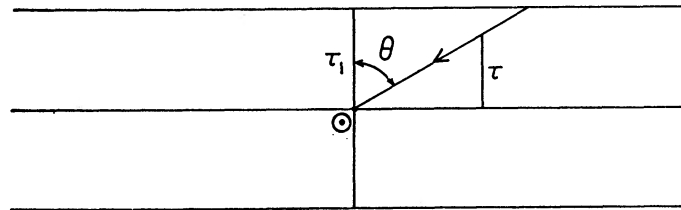


FIG. 2.—Sketch illustrating the symbols used in the radiative-transfer model of the Galaxy

be governed by a phase function $\Phi(\alpha)$ and let the ratio of stellar emission per unit volume into unit solid angle to the extinction coefficient per unit distance be denoted by a . The total intensity I —the sum of the intensity of starlight I_0 and the intensity of the scattered light I_1 —follows then from the equation of transfer

$$\mu \frac{dI}{d\tau} = I - \int I \Phi(\alpha) d\omega - a, \quad (1)$$

where $\mu = \cos \theta$ and where τ is measured from the central plane. Likewise, for the starlight

$$\mu \frac{dI_0}{d\tau} = I_0 - a. \quad (2)$$

Equation (2) has the formal solution

$$I_0 = \frac{1}{\mu} \exp\left(\frac{\tau}{\mu}\right) \int_{\tau}^{\tau_1} a \exp\left(-\frac{\tau'}{\mu}\right) d\tau', \quad (3)$$

provided

$$0 < \mu < 1.$$

Assuming a constant value of a throughout the system, we find for the integrated starlight as a function of galactic latitude as seen at $\tau = 0$,

$$I_0 = a \left[1 - \exp\left(-\frac{\tau_1}{\mu}\right) \right]. \quad (4)$$

Since we have for the DGR

$$I_1 = I - I_0, \quad (5)$$

a solution of equation (1) combined with equation (4) would permit us to calculate the intensity of the scattered light, once the values for a and τ_1 are known for the observed regions of the Milky Way and the phase function $\Phi(\alpha)$ is specified. An analytical solution to this problem has been obtained by Henyey and Greenstein (1941) for the two-parameter phase function

$$\Phi = \gamma(1 - g)/4\pi + \gamma g \Psi \quad (6)$$

under assumption of a constant a and within the validity of Eddington's approximation. With γ we denote the albedo of the scattering particles, with g the asymmetry factor of the phase function. Ψ is a perfectly forward-throwing phase function of unit albedo. By definition, g is the weighted mean of the cosine of the scattering angle with the phase function of unit albedo as weighting function. We can verify that $\Phi(\alpha)$ satisfies the condition

$$\int \Phi(\alpha) \cos \alpha d\omega = g \quad (7)$$

for $\gamma = 1$. Thus, by varying g between $+1$ and -1 we can represent phase functions ranging from completely forward-throwing to completely backward-throwing ones with an isotropic phase function for $g = 0$.

Henyey and Greenstein (1941) find the approximate solution for the DGR

$$I_1 = \frac{a}{1-\gamma} \left\{ \gamma + (1-\gamma) \exp\left(-\frac{\tau_1}{\mu}\right) - \exp\left[-\frac{\tau_1(1-\gamma g)}{\mu}\right] - \frac{\gamma(1-g)}{(1-\gamma g)} \right. \\ \left. \times \frac{1 - \exp[-\tau_1(1-\gamma g)/\mu] [\cosh p\tau_1 + (p\mu \sinh p\tau_1)/(1-\gamma g)]}{[1 - 3(1-\gamma)\mu^2/(1-\gamma g)] [\cosh p\tau_1 + (\frac{2}{3}p \sinh p\tau_1)/(1-\gamma g)]} \right\}, \quad (8)$$

where

$$p = \sqrt{[3(1 - \gamma)(1 - \gamma g)]}. \quad (9)$$

It should be noted that equation (8) is derived under quite general assumptions with respect to the density distribution of the matter and that a constant value of a in a homogeneous plane-parallel slab model with finite vertical optical thickness is by no means equivalent to a constant-density model. As shown in Figure 3, our assumptions are satisfied by models with quite realistic distributions of stars and interstellar dust.

Before we can make use of equation (8) effectively, however, the values of a and τ_1 as function of band-pass wavelength will have to be determined. They depend on the

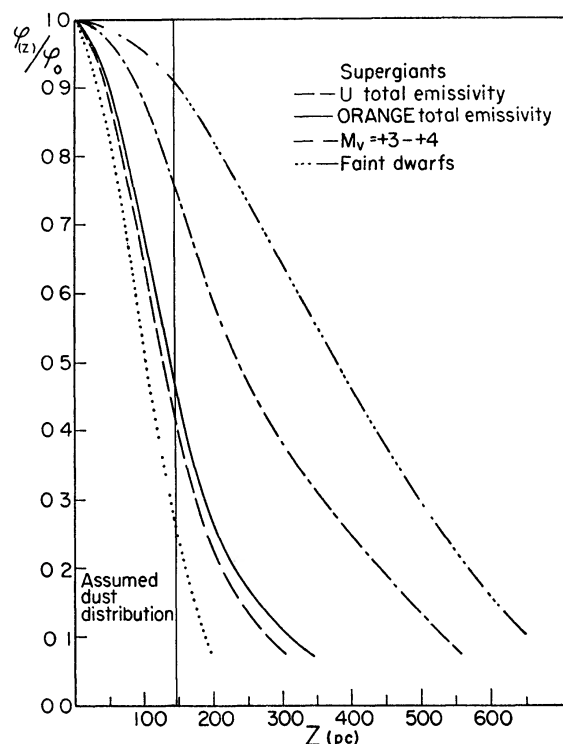


FIG. 3.—Relative density distribution of interstellar dust and various star types with height z above the galactic plane as used in the Galaxy model.

definition of the magnitude system used, on the amount of interstellar extinction present with its known wavelength dependence, and on the variation of the luminosity function with height above the plane of the Galaxy. Therefore, the second aspect of the Galaxy model deals with the effects which these circumstances have on the intensity and distribution of the integrated starlight in the three band passes.

For this detailed study we adopt the luminosity function as given by Schmidt (1959) and arrange the stars in exponential distributions around the central plane with equivalent widths as quoted by Schmidt. Since in the real Galaxy the distribution of interstellar dust is quite irregular in the form of individual clouds, it appeared that the assumption of a homogeneous dust layer of a given thickness and constant density was of the same quality as a dust layer resulting from the requirement of a constant value of a throughout the system. Therefore, the former was adopted because of its greater mathematical simplicity and thicknesses of the layer between 220 and 290 pc were assumed. The density was specified by fixing the amount of total extinction per parsec at the effective wavelength of the B filter. The interstellar reddening curve was used for

scaling the extinction for the three band passes, and using standard colors of the *UBV* system by Johnson (1963) and the author's calibration measurements with the *ORANGE* filter, Schmidt's M_V luminosity function was transformed into functions expressed in terms of M_B , M_U , and M_{ORANGE} .

From these data it was possible to derive numerically the frequency function of apparent magnitudes $A(m, b^{\text{II}})$ for a specified direction b^{II} by integrating

$$A(m, b^{\text{II}}) = \int_{-\infty}^{\infty} (1/\phi_0) F(y, b^{\text{II}}) L_M(m - y) dy, \quad (10)$$

where

$$y = 5 \log(r/10) + e(r), \quad (11)$$

with $e(r)$ expressing the amount of interstellar extinction encountered by a star at distance r from the Sun in direction b^{II} . L_M is the known luminosity function, ϕ_0 is the number of stars per cubic parsec in the plane of the Galaxy. $F(y, b^{\text{II}})dy$ represents the number of stars within a solid angle of one square degree and between the distance

TABLE 3
BRIGHTNESS RATIOS OF THE INTEGRATED
STARLIGHT AS FUNCTION OF
GALACTIC LATITUDE

b^{II}	$n(U)/n(B)$	$n(\text{ORANGE})/n(B)$
0° ..	0.94	2.94
5	0.96	2.84
10	0.99	2.76
20	1.00	2.72
30	1.00	2.71
40 .	1.00	2.71

limits $y \pm dy/2$. This function can be obtained for every direction from the assumed number density distributions for the different types of stars

$$\phi(z, M) = \phi_0(M) \exp[-\pi z^2/4h^2(M)], \quad (12)$$

where $h(M)$ is identical with the equivalent half-thicknesses to be derived from Schmidt's tables.

The integrated brightness of all stars contained in a solid angle of one square degree expressed in units of 10th magnitude stars in the respective band pass is then obtained from the integral

$$I_0(b^{\text{II}}) = \int_{-\infty}^{\infty} A(m, b^{\text{II}}) \times 10^{-0.4(m-10.0)} dm. \quad (13)$$

The primary results of these computations are the ratios of the integrated brightness of starlight in three band passes as functions of galactic latitude. It was found that these ratios depend nearly exclusively on the shape of the three luminosity functions and their variations with height above the plane as well as on the wavelength dependence of the interstellar extinction. It is a fortunate circumstance that the ratios are relatively insensitive to changes in the density of interstellar dust, although the individual integrated brightnesses depend strongly on the latter. The ratios which will allow us to determine a and τ_1 for the *U* and *ORANGE* band passes once the corresponding values for *B* are known are listed in Table 3. They are valid for average interstellar extinctions between 1 mag/kpc and 2 mag/kpc in the *B* band pass.

The values of a and τ_1 for B are found in the following manner. In equation (4) the integrated starlight is expressed in terms of these two parameters. We therefore take values of the integrated starlight as functions of galactic coordinates of the observed fields in Cygnus and Tau-Aur, as they are provided by Roach and Megill (1961) based on the star counts in *Groningen Publication No. 43*, correct these for stars brighter than $m_{pg} = 6$, which are omitted there, and transform to units used in this paper by $n(B) = 0.903n(pg)$. We then fit equation (4) to the intensity distribution thus obtained and derive the appropriate values of a and τ_1 .

Although the Roach-Megill tables give only a very smoothed representation of the Milky Way appearance, they should fairly well yield the average illumination of the interstellar particles along a line of sight of about 1500-pc length, since this is what the parameters a and τ_1 are intended to describe.

For scaling of a for the other two band passes we use the ratios contained in Table 3; the changes in τ_1 follow from the variation in the profile of the integrated starlight with wavelength and the dependence of optical depth in the dust with the band pass. Table 4 contains the final values.

TABLE 4
STAR DISTRIBUTION PARAMETERS

REGION	U		B		ORANGE	
	a	τ_1	a	τ_1	a	τ_1
Cygnus	160	0 17	170	0 155	500	0 12
Taurus-Auriga	103	0.18	110	0 16

The problem of scaling τ_1 with wavelength is closely connected with the assumption of a constant value of a throughout the system for a given band pass. In fact, if we assume a constant a for B , the circumstance that our Galaxy model includes a variation of the luminosity function with height z above the central plane requires—according to the definition of a —that for U the value of a decreases with increasing z while for ORANGE a increases with increasing z . This is a second-order effect only, but it has been taken into account in the determination of the τ_1 values in Table 4 such that constant a values can be maintained.

In Figure 3 the assumed distribution of characteristic types of stars is shown for our model and the profiles of the total emissivity of all stars in U and ORANGE are included; these last two curves indicate the required dust distributions for the respective band passes for constant values of a . The adopted dust distribution is intermediate, and can be approximated by a homogeneous layer of equivalent height of 145 pc and constant density in its integrated effects when dealing with the second aspect of the model.

With the material available a series of other studies could be performed. In order to see whether the presently uncertain knowledge concerning the faint end of the luminosity function could influence our estimate of faint-star background we determined the contribution to the integrated light of stars fainter than $V = 20$ by stars of different absolute magnitudes. It was found that under average conditions of interstellar extinction of about 1.5 mag B/kpc stars between $M_V = 0$ and $M_V = +7$ with a maximum near $M_V = +4$ contribute the bulk of faint starlight. The space density of stars of $M_V > +7$ would have to be larger by several orders of magnitude in order to seriously affect our results. This, however, appears to be very unlikely.

We then investigated under what conditions the faint stars of $V > 20$ could at all become detrimental. The study indicates that there is danger of contamination in direc-

tions close to the galactic equator with an average extinction coefficient less than 0.5 mag_B/kpc, i.e., regions of high transparency like the Cygnus cloud. For average or above average extinction, as we find it in the Taurus dust complex and the Cygnus rift, however, the contamination of the DGR measurements by faint stars is small and can easily be taken into account in the reductions.

At this point also the integrated light from stars brighter than $m_{pg} = 6$ was determined as a function of galactic latitude and extinction, which had to be added to the integrated *Groningen Publication No. 43* star counts, since it is the total light of all stars which serves as illuminating source and should be represented by equation (4). The contribution of stars brighter than $m_{pg} = 6$ relative to those fainter increases with galactic latitude, thus causing a broader distribution of intensity I_0 over galactic latitude and hence increasing τ_1 . The relative contribution of bright stars also increases with increasing extinction. This result was of special importance in the proper determination of the star-background parameters a and τ_1 in Taurus.

The systematic difference between the star counts at low galactic latitudes in *Groningen Publication No. 43* (GR 43) and those in *Mount Wilson Contribution No. 301* (MW 301) will not be discussed here; the former are the more frequently accepted and have been adopted throughout this paper for the determination of the star background parameters. We will later point out the consequences which would have resulted from the adoption of the *Mount Wilson Contribution No. 301* star counts.

With a fairly reliable set of values of a and τ_1 we can proceed now to derive the scattering parameters γ and g by comparing the observations contained in Figure 1 with the predictions from equation (8). Several possible methods are available. Their relative worth will be judged on the basis of how sensitive they are to the observational uncertainties, especially to the fact that the intensities plotted in Figure 1 are only lower limits to the absolute values.

Henyei and Greenstein (1941) employ the method of the relative concentration of diffuse radiation and starlight measured by the parameter

$$\sigma = \frac{I_1(b^{\text{II}} = 0^\circ) - I_1(b^{\text{II}} = 20^\circ)}{I_1(b^{\text{II}} = 0^\circ)} - \frac{I_0(b^{\text{II}} = 0^\circ) - I_0(b^{\text{II}} = 20^\circ)}{I_0(b^{\text{II}} = 0^\circ)} \quad (14)$$

to obtain the most probable combinations of γ and g , after deriving an independent value of γ from the intensity of the DGR at the galactic equator. Theoretically, the parameter σ depends most drastically on g and far less on γ ; the determination of σ from the observational data leads not only to an overestimate from the first half of the right-hand side of equation (14) but also to an increased error margin because of the uncertainties in the distribution of the integrated starlight I_0 . Consequently, this method results in a greatly overestimated value of g and a rather uncertain value of γ .

A second method, which avoids use of the integrated starlight, follows from the fact that the intensity of the DGR depends on γ and g in a different way for different galactic latitudes. One finds that at higher latitudes, say at $b^{\text{II}} = 20^\circ$, the intensity is nearly exclusively determined by the albedo γ while close to the galactic equator the asymmetry g of the phase function strongly influences the intensity. Theoretically, therefore, from two single observations at $b^{\text{II}} = 0^\circ$ and $b^{\text{II}} = 20^\circ$ one could determine in a γ - g diagram two solutions which would intersect at a point, indicating the correct values of the two parameters γ and g . However, the intensities in Figure 1 are too small by a constant amount. The relative inaccuracy at $b^{\text{II}} = 0^\circ$ is only small; that solution would therefore be quite adequate; at $b^{\text{II}} = 20^\circ$ the relative error is substantial, resulting in a wrong solution and hence a wrong intersection. The results of this method applied to our observations are a greatly underestimated albedo γ and a value of g which is too large.

A third method, which was that finally adopted, was one which did not require the knowledge of the absolute DGR intensities and at the same time made use of all the

available observations, not merely the results at selected latitudes. Here, the intensities of the DGR at galactic latitudes ranging from $b^{\text{II}} = 0^\circ$ to $b^{\text{II}} = 27^\circ$, for a given set of values (γ, g) , were computed with the help of equation (8). The resulting curves were then treated exactly like the observations, and a zero level at $b^{\text{II}} = 27^\circ$ was introduced. The intensities above this level were compared with the observations directly.

The uncertainties of this method result only from the approximate nature of the Galaxy model and the observational scatter of the data, and it should therefore be considered superior to the previously discussed methods. A difficulty which could make this method rather time-consuming, however, is the large number of possible combinations of g and γ . It was therefore decided to take those (γ, g) combinations which apply to the most widely discussed models of interstellar dust particles and thus have an immediate comparison of the predictions of these models and the actual observations.

The models considered were those of spherical particles consisting of dirty ice, pure graphite, graphite covered with a shell of dirty ice, and finally Platt particles. For the three classically scattering models Mie computations for spherical isotropic grains were carried out and size distributions of these were determined with the interstellar reddening curve as a criterion which had to be satisfied. For individual particles we compute efficiencies for extinction, scattering, absorption, and radiation pressure, Q_{ext} , Q_{sca} , Q_{abs} , and Q_{rpr} , respectively, and then find

$$\gamma = Q_{\text{sca}}/Q_{\text{ext}} \quad (15)$$

and

$$g = (Q_{\text{ext}} - Q_{\text{rpr}})/Q_{\text{sca}}. \quad (16)$$

If $n(r)$ expresses the size distribution of particles with different radius r the corresponding average values of γ and g are obtained from

$$\langle \gamma \rangle = \int Q_{\text{sca}} \pi r^2 n(r) dr / \int Q_{\text{ext}} \pi r^2 n(r) dr \quad (17)$$

and

$$\langle g \rangle = \int g Q_{\text{sca}} \pi r^2 n(r) dr / \int Q_{\text{sca}} \pi r^2 n(r) dr. \quad (18)$$

It should be noted that since both g and Q_{sca} increase with size in the range of radii which we are considering here, $\langle g \rangle$ is especially sensitive to the fraction of larger particles in a size distribution. If $\langle g \rangle$ is found to be small—say, close to zero—this could be an indication that only very small particles are present.

The Mie calculations involving graphite are made with the optical constants measured for the case where the electrical vector of the incident radiation lies in the basal plane of a graphite crystal. In this plane the conductivity is about two orders of magnitude larger than in the direction perpendicular to it. The light scattered by a single graphite flake, therefore, will have a strongly asymmetric phase function with an intensity maximum along the axis of symmetry of the grain perpendicular to the basal plane, not at all corresponding to the g -value derived from Mie theory. For a cloud of randomly oriented graphite flakes, however, one should expect $g \simeq 0$.

The albedo γ of graphite particles should follow fairly correctly from the Mie calculations, since the faces of graphite flakes parallel to the basal planes present a much larger cross-section to the incident light than the edges of the flakes, so that the amount of light scattered and absorbed should be determined by the optical properties existing parallel to the planes.

For Platt particles nothing definite is known with regard to γ - and g -values, since no quantitative theory exists for these particles. Platt (1956) concludes that they have a near unit albedo and an isotropic phase function and for the sake of comparison we accept these properties. In Table 5 we list for the three band passes the properties of the models tested.

IV. DISCUSSION

In Figure 4, *a-e*, we have superimposed the observational points with model DGR distributions which were derived according to the third method described above. In Cygnus the theoretical curves are shifted to positive galactic latitudes by 3° to take into account the deviations from symmetry in that part of the Milky Way. In comparing the intensity, distribution over galactic latitudes, and wavelength dependence of the intensity of the DGR with the theoretical predictions we can immediately exclude pure graphite and dirty ice as scatterers in interstellar space.

Graphite particles of the size satisfying the reddening curve have an albedo too low to produce a sufficient amount of diffuse light. The comparison becomes even worse for graphite when the more realistic value of $g = 0$ for clouds of graphite flakes is assumed,

TABLE 5
ALBEDO AND ASYMMETRY FACTOR OF THE SCATTERING PHASE
FUNCTION FOR VARIOUS PARTICLE MODELS

Model	$\lambda(\text{\AA})$	$\langle \gamma \rangle$	$\langle g \rangle^*$
Dirty ice, Oort-van de Hulst distr. $n=1.33-0.05i$, $r_H=$ 0.125μ	3597	0 73	0 76
	4348	.69	.71
	6100	.60	.58
Graphite, Wickramasinghe equilib. distr. $r_H=0.012 \mu$	3597	.39	.23 (0 00)
	4348	.35	.18 (.00)
	6100	.26	.12 (.00)
Graphite+dirty ice, core radius 0.03μ , equilib. distr. of mantles, $P/\mu=15.0$	3597	.53	.51 (.28)
	4348	.47	.40 (.22)
	6100	.34	.21 (0 09)
Platt particles	3597	.98	.00
	4348	.98	.00
	6100	0 98	0 00

* Values in parentheses correspond to graphite in form of flakes.

since this leads to a reduced intensity at the galactic equator. The strongly forward-throwing phase function of dirty ice combined with a relatively high albedo would produce diffuse radiation in the vicinity of the galactic equator with an intensity exceeding that of the integrated light of all stars in the same region, therefore far in excess of the observed amount. Fairly reliable surface photometries of the night sky support this argument against the dirty-ice model, since they demonstrate that this amount of excess light is definitely not present.

The evaluation of the composite model consisting of graphite cores and dirty-ice shells is more difficult. However, the *U* and ORANGE measurements in Cygnus reveal that this model also does not explain the observed DGR distributions, when its g -value is computed by the classical Mie theory. When the lower g -values for graphite flakes surrounded by dirty ice are accepted, the comparison improves for *U* but it deteriorates for ORANGE due to the low albedo in this band pass and especially the relatively high DGR intensity at higher galactic latitudes ($b^{\text{II}} > 10^\circ$) remains unexplained.

The composite model has been favored recently since it seems to solve problems such as the high interstellar extinction in the far-ultraviolet and the wavelength dependence of interstellar polarization, and since it has a larger albedo than pure graphite. Unless its scattering properties are totally different from those assumed here, the composite model is not supported by the DGR data, however.

The result of a detailed comparison is the unexpected feature that an isotropic

scatterer with albedo near unity in all three band passes is the best solution for both regions of the Galaxy which were observed. These scattering properties are not to be found in those classically scattering particles satisfying the interstellar reddening curve, but are generally associated with quantum mechanically scattering particles first suggested by Platt (1956).

One consequence of an isotropic phase function is a very broad distribution of the DGR which is observed and the fact that there is still a substantial amount of scattered light present even at $|b^{\text{II}}| = 27^\circ$. Adding these amounts to the observed intensities we arrive at new, now absolute, zero levels and can thus estimate the absolute intensities of the DGR at different latitudes. The maximum values of the DGR intensities predicted on this basis and the intensities at $|b^{\text{II}}| = 25^\circ$ are listed in Table 6. Since star counts at a latitude of $|b^{\text{II}}| = 25^\circ$ are fairly reliable, a precise surface photometry including starlight and diffuse light in these areas should reveal this excess intensity.

Using the intensities in Table 6 we can compute the colors of the DGR. Expressed in the *UBV* system we obtain for Cygnus at the galactic equator: $U - B = -0.05$, $B - V = +0.57$, and for $|b^{\text{II}}| = 25^\circ$: $U - B = -0.10$, $B - V = +0.44$. The decrease of

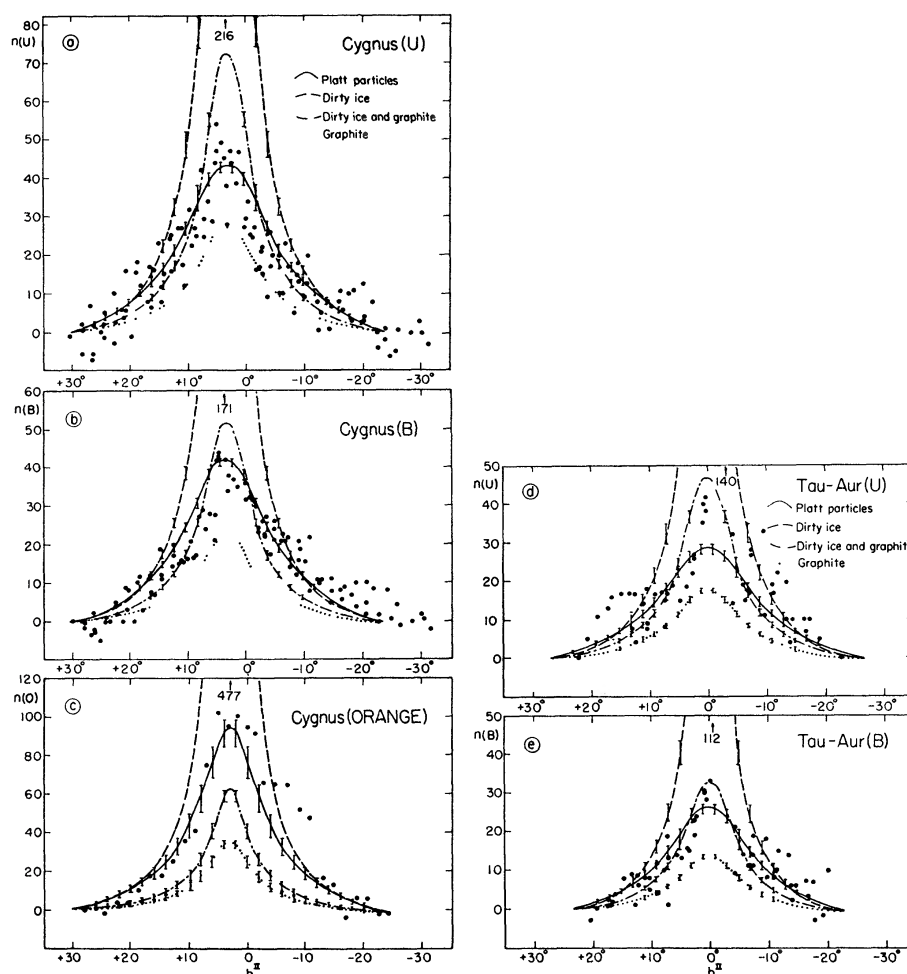


FIG. 4.—Comparison of theoretical and observed DGR intensity distributions. The vertical bars indicate the uncertainty of the theoretical predictions due to probable errors in the determination of α and τ_1 .

the color indices with increasing galactic latitude is caused primarily by the pronounced dependence of optical thickness in the line of sight on wavelength. It is aided by the decrease of the color indices of the integrated starlight with increasing galactic latitude. These are for Cygnus $U - B = +0.07$ and $B - V = +0.73$ for $b^{\text{II}} = 0^\circ$, and $U - B = 0.00$ and $B - V = +0.68$ for $|b^{\text{II}}| = 25^\circ$, as obtained with the ratios contained in Table 3.

It was investigated whether any of the stated conclusions would be subject to change if we had adopted the MW301 star counts instead of GR43 counts for the derivation of the star background parameters. In general, we would have found lower values of a , partially balanced by higher values of τ_1 . For example, in Cygnus we would have had for the B band pass $a = 105$, $\tau_1 = 0.22$. The result of this study was that even under these conditions the Platt particles, among all other models discussed, provided the best agreement with the observations. The decision is not quite as obvious as in the case where the GR43 counts are used; however, there are two strong arguments indicating that the use of the GR43 counts was justified. First, independent star counts in Cygnus by Miller and Hynek (1939) and in Taurus by McCuskey (1938) agree much better with GR43; second, in comparing GR43 counts for specific regions with recent photoelectric sky photometry by Roach and Smith (1964) one finds that their integrated total light in

TABLE 6
FINAL INTENSITIES OF THE DGR

b^{II}	$n(U)$		$n(B)$		$n(\text{ORANGE})$	
	0°	25°	0°	25°	0°	25°
Cygnus	61 ± 6	20	58 ± 6	18	120 ± 15	30
Taurus-Auriga	42 ± 5	14	39 ± 5	12

the visual band pass is 1.26 times that predicted by the star counts (Roach 1964). Adding our DGR intensities to the integrated starlight obtained from GR43, we find for the V band a factor of 1.28 ± 0.02 . In the case of the MW301 counts, a factor of 1.46 ± 0.03 would have resulted instead.

We conclude, therefore, on the basis of our observations that particles with an albedo near unity and an isotropic phase function, properties which are assumed to be realized in Platt particles, are the most likely candidates for interstellar scatterers. We find supporting evidence for this statement in several independent observations.

Recently Roach (1967) has completed a study of the diffuse galactic light based on extensive observational material with a wide-field sky photometer. Using values of the integrated starlight based on the average of GR43 and MW301 he gives the ratio of diffuse galactic light to line-of-sight starlight as function of galactic latitude averaged over galactic longitudes. In Figure 5, Roach's results are given for two values of the airglow together with the B measurements of the present investigations reduced with a star background as obtained from the parameters contained in Table 4. Also included are the curves predicted for the four basic models of interstellar particles studied previously, using the same line-of-sight starlight as for our observations. Considering the different observational methods employed by Roach and the author, the agreement is surprisingly good. The fact that only an isotropic scatterer with unit albedo explains the combined data becomes even more obvious than in Figure 4.

Numerous investigations of reflection nebulae, the most recent and extensive one by Dorschner and Gürtler (1966), also indicate that the albedo of the scattering medium is close to unity in the red as well as in the blue region of the spectrum, whereby an iso-

tropic phase function is implicitly assumed. There has never been any evidence that the dust particles in reflection nebulae are physically different from those in the general interstellar space, although this argument has been frequently used. Now it rather appears that they have identical scattering properties.

Reliable photoelectric data of the surface brightness of the reflection nebula surrounding Merope as function of distance from the illuminating star were reported by O'Dell (1965) for four band passes. Greenstein's (1951) approach for computing the surface brightness of a reflection nebula was used to derive lower limits for the albedo of the scattering medium with the result that γ is larger than 0.9 over the wavelength range

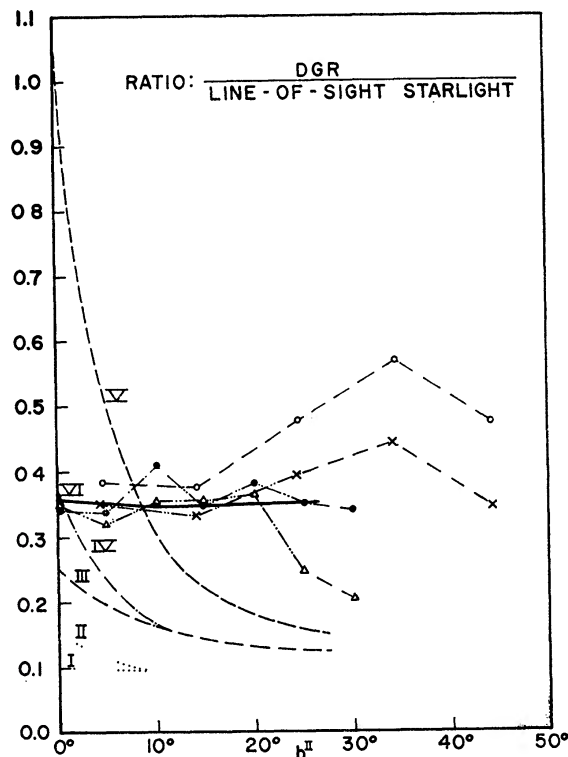


FIG. 5.—Comparison of DGR observations with proposed models. Models: I, graphite flakes; II, spherical isotropic graphite particles; III, graphite flakes with ice coating; IV, spherical graphite particles with ice shell; V, spherical dirty ice particles; VI, Platt particles. Observations: *open triangles*, Witt, Taurus-Auriga; *filled circles*, Witt, Cygnus; *crosses*, Roach I; *open circles*, Roach II.

from $\lambda 5620$ to $\lambda 3400$ Å. Considering the fact that the star Merope lies in front of the nebula with respect to the observer, a forward-throwing phase function must be excluded in light of the high albedo.

If we now assume that the wavelength dependence of the scattering efficiency of the medium is to a good approximation identical to the wavelength dependence of interstellar extinction, which should be true in the case of a high albedo, we can also reproduce from theory the color-excess curves observed by O'Dell for different regions of the Merope nebula, again using Greenstein's approach. Internal reddening and variation of optical thickness with wavelength are sufficient to explain the detected color changes with distance from the star. An isotropic phase function and a wavelength-independent albedo had to be assumed here.

The radar scattering curve, which was suggested by Krishna Swamy and O'Dell (1967) as a new tool for testing models of interstellar grains when applied to the Merope nebula,

requires a small optical depth effect in a plane-parallel nebula of finite optical thickness, provided the scattering particles have an albedo close to unity and an isotropic phase function. Again, the wavelength dependence of the scattering efficiency must be derived from the interstellar reddening curve. A perfect agreement between predictions based on Chandrasekhar's (1950) treatment of diffuse reflection and transmission for isotropic scattering with the observed radar curve can be achieved when one assumes that the albedo decreases slightly with increasing wavelength, e.g., $\gamma_{3400} = 1.00$ and $\gamma_{5620} = 0.90$, but even the predicted radar scattering curve for constant albedo agrees better with the observations than the classical particle models tested by Krishna Swamy and O'Dell.

A further test based on the distribution of the total light in the Milky Way at the wavelengths $\lambda\lambda 2100, 2500$, and 2800 \AA will be described in a forthcoming publication (Lillie and Witt, in preparation). A preliminary analysis strongly indicates that an isotropic phase function will be required to explain the observations in the extreme ultraviolet.

Even without this additional supporting evidence the observations of the DGR reported in this paper and the large-scale properties of the Galaxy model employed are accurate enough to suggest strongly the presence in interstellar space of dust particles having an albedo close to unity and an isotropic phase function. These scattering properties are characteristic of Platt particles, although there may be other particle types, not considered at this time, that also possess these properties.

Some interesting implications follow from this conclusion. If the particles are just molecular structures of a size smaller than 20 \AA , it seems possible that diffuse interstellar absorption lines, not yet definitely identified, originate in the same particles by electron transitions. The lines therefore could turn out simply to be a fine structure of the interstellar reddening law.

An important implication of our conclusion is also the fact that the infrared radiation at wavelengths greater than 10μ , which is predicted for classical interstellar particles by Stein (1966), should not be present provided the particles are exclusively of the Platt type. For these we expect absorption and re-emission at the same frequency, hence no heating would occur.

Finally, it will be important to understand theoretically the physical principles behind the scattering process, in order that the scattering efficiencies of the particles and the wavelength dependence of the polarization of starlight passing through a cloud of Platt particles can be numerically predicted. Also, the chemical nature of the particles should be investigated both through a theoretical approach to their process of formation and through systematic studies of diffuse interstellar lines.

I wish to thank Dr. C. R. O'Dell for suggesting this investigation and for his continued advice and encouragement during the course of this work. A helpful discussion on radiative-transfer problems with Dr. D. N. Limber is gratefully acknowledged. I am also very much obliged to Dr. F. E. Roach for making available to me his independent observations of the diffuse galactic light before publication, and I wish to thank an unknown referee for some clarifying remarks on the scattering properties of graphite flakes.

The research reported in this paper was supported by the National Science Foundation with grant GP-5155.

REFERENCES

- Ashburn, E. V. 1954, *J. Atm. Terr. Phys.*, **5**, 83.
 Chandrasekhar, S. 1950, *Radiative Transfer* (Oxford: Clarendon Press).
 Dorschner, J., and Gürtler, J. 1966, *Astr. Nach.*, **289**, 57.
 Elsässer, H., and Haug, U. 1960, *Zs. f. Ap.*, **50**, 121.
 Elsässer, H., and Siedentopf, H. 1957, *Zs. f. Ap.*, **43**, 132.
 Elvey, C. T., and Roach, F. E. 1937, *Ap. J.*, **85**, 213.
 Greenstein, J. L. 1951, *Astrophysics*, ed. J. A. Hynek (New York: McGraw-Hill Book Co.), chap. xiii.

- Heney, L. G., and Greenstein, J. L. 1941, *Ap. J.*, **93**, 70.
Houten, C. J. van. 1961, *B.A.N.*, **16**, 1.
Johnson, H. L. 1963, *Basic Astronomical Data*, ed. K. Aa. Strand (Chicago: University of Chicago Press), chap. xi.
Krishna Swamy, K. S., and O'Dell, C. R. 1967, *Ap. J.*, **147**, 937.
Lillie, C. F., and Witt, A. N. 1968 (in preparation).
Lynds, B. T. 1962, *Ap. J. Suppl.*, Vol. 7, No. 64.
McCuskey, S. W. 1938, *Ap. J.*, **88**, 209.
Miller, F. D., and Hynek, J. A. 1939, *Perkins Obs. Contr.*, No. 13.
O'Dell, C. R. 1965, *Ap. J.*, **142**, 604.
Platt, J. R. 1956, *Ap. J.*, **123**, 486.
Roach, F. E. 1957, *Modern Astrophysics* (Paris: Gauthier-Villars), pp. 49–66.
———. 1964, *Space Sci. Rev.*, **3**, 512.
Roach, F. E., and Megill, L. R. 1961, *Ap. J.*, **133**, 228.
Roach, F. E., and Smith, L. L. 1964, *N.B.S. Tech. Note*, No. 214.
Schmidt, M. 1959, *Ap. J.*, **129**, 243.
Smith, L. L., Roach, R. E., and Owen, R. W. 1965, *Planet. and Space Sci.*, **13**, 207.
Stein, W. 1966, *Ap. J.*, **144**, 318.
Wang, S.-K. 1936, *Pub. Obs. Lyon*, Vol. 1, No. 19.

Copyright 1968. The University of Chicago. Printed in U S.A.